Ricin A-Chain Substrate Specificity in RNA, DNA, and Hybrid Stem-Loop Structures

ARTICLE *in* BIOCHEMISTRY · MAY 2004

Impact Factor: 3.02 · DOI: 10.1021/bi0498508 · Source: PubMed

2 AUTHORS, INCLUDING:

Timothy K Amukele
Johns Hopkins University
18 PUBLICATIONS **114** CITATIONS

SEE PROFILE

Articles

Ricin A-Chain Substrate Specificity in RNA, DNA, and Hybrid Stem−Loop Structures†

Tim K. Amukele and Vern L. Schramm*

Department of Biochemistry, Albert Einstein College of Medicine, 1300 Morris Park Avenue, Bronx, New York 10461

Received January 20, 2004; Revised Manuscript Received February 25, 2004

ABSTRACT: Ricin toxin A-chain (RTA) is the catalytic subunit of ricin, a heterodimeric toxin from castor beans. Its ribosomal inactivating activity arises from depurination of a single adenine from position A^{4324} in a GAGA tetraloop from 28S ribosomal RNA. Minimal substrate requirements are the GAGA tetraloop and stem of two or more base pairs. Depurination activity also occurs on stem−loop DNA with the same sequence, but with the k_{cat} reduced 200-fold. Systematic variation of RNA 5′-$G_1C_2G_3C_4[G_5A_6G_7A_8]$-$G_9C_{10}G_{11}C_{12}$-3′ 12mers via replacement of each nucleotide in the tetraloop with a deoxynucleotide showed a 16-fold increase in k_{cat} for $A_6 \rightarrow dA_6$ but reduced k_{cat} up to 300-fold for the other sites. Methylation of individual 2′-hydroxyls in a similar experiment reduced k_{cat} by as much as 3×10^{-3}-fold. In stem−loop DNA, replacement of d[$G_5A_6G_7A_8$] with individual ribonucleotides resulted in small kinetic changes, except for the $dA_6 \rightarrow A_6$ replacement for which k_{cat} decreased 6-fold. Insertion of d[$G_5A_6G_7A_8$] into an RNA stem−loop or $G_5A_6G_7A_8$ into a DNA stem−loop reduced k_{cat} by 30- and 5-fold, respectively. Multiple substitutions of deoxyribonucleotides into RNA stem−loops in one case (dG_5,dG_7) decreased k_{cat}/K_m by 10^5-fold, while a second change (dG_5,dA_8) decreased k_{cat} by 100-fold. Mapping these interactions on the structure of GAGA stem−loop RNA suggests that all the loop 2′-hydroxyl groups play a significant role in the action of ricin A-chain. Improved binding of RNA−DNA stem−loop hybrids provides a scaffold for inhibitor design. Replacing the adenosine of the RTA depurination site with deoxyadenosine in a small RNA stem−loop increased k_{cat} 20-fold to 1660 min^{-1}, a value similar to RTA's k_{cat} on intact ribosomes.

Enzymes and chemical catalysts enhance reaction rates by reducing the energetic barrier to the transition state. Enzymes can use interactions that are distant from the site of the chemical transformation to reduce the barrier and can demonstrate exquisite discrimination between substrates that are chemically or structurally similar. These qualities are related. As shown in the analysis of Albery and Knowles (*1*), specific binding in a portion of the substrate that does not undergo a chemical transformation can still decrease the catalytic barrier independent of chemical group catalysis. Our studies with RNA stem−loop substrate specificity will be explored with this and related chemical reactivity concepts.

RTA[1] is the catalytic subunit of ricin, an extremely toxic heterodimeric (type II) ribosomal inhibitory protein (RIP) that mediates its cytotoxicity by depurinating a conserved adenosine, A^{4324} of the 28S rRNA subunit (rat), thereby destroying an elongation factor binding site and ablating translation (*2*, *3*). The ribosomal site of RTA-catalyzed depurination is a GAGA tetraloop stem−loop structure. Smaller stem−loops that retain the GAGA tetraloop sequence are also substrates for RTA (*4*). In addition, DNA stem−loops that retain the GAGA loop sequence are also substrates for RTA (*5*). Characterization of RNA and DNA 10mer substrates (3 bp stem and tetraloop) showed that the RNA substrate underwent turnover at 10 times the rate of the DNA substrate. However, the intrinsic reactivity of purine 2′-deoxy- versus purine ribonucleosides to acid-catalyzed depurination ($k_{deoxyadenosine}/k_{adenosine}$) is 760 (*6*). RTA catalysis of stem−loop oligonucleotide depurination proceeds via a mechanism similar to the acid-catalyzed process, i.e., an S_N1 mechanism with formation of an oxacarbenium ion followed by addition of water in a separate step (*7*, *8*). The reason for the discrepancy between the relative rates of enzyme catalysis of A10 and dA10 and the intrinsic reactivity of their constituent nucleosides is not known. In this study, we attempt to define structural correlates for this phenomenon by kinetically characterizing RNA−DNA hybrid GAGA tetraloop stem−loops containing a single deoxyribonucleo-

† This work was supported by NIH Grant CA72444 and Training Grant GM07288. We thank Dr. Haiteng Deng of the Laboratory of Macromolecular Analysis and Proteomics (Albert Einstein College of Medicine) for mass spectrometry analysis.

* To whom correspondence should be addressed. Telephone: (718) 430-2813. Fax: (718) 430-8565. E-mail: vern@aecom.yu.edu.

[1] Abbreviations: RTA, ricin toxin A-chain; A12, RNA 5′-G_1C_2-$G_3C_4G_5A_6G_7A_8G_9C_{10}G_{11}C_{12}$-3′; dA12, DNA d(5′-GCGCGAGAGCGC-3′); RIP, ribosomal inhibitory protein; A10, RNA 5′-$C_1G_2C_3G_4A_5G_6A_7$-$G_8C_9G_{10}$-3′; dA10, DNA d(5′-CGCGAGAGCG-3′); OMeRNA, RNA with 2′-*O*-methyl groups; GNRA, tetraloop sequence in which N is any nucleoside and R is purine; TS, transition state.

10.1021/bi0498508 CCC: $27.50
Published on Web 04/09/2004

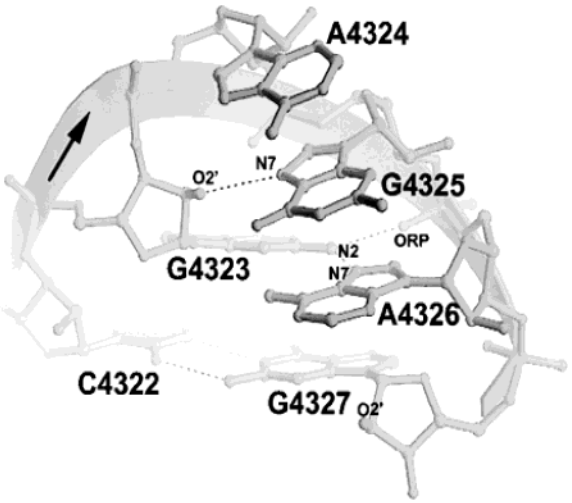

FIGURE 1: This figure is from ref *29*. Copyright 1998 National Academy of Sciences. Used with permission. It highlights the interactions that have been shown to be involved in stabilization of GAGA hairpins. The first and fourth loop residues are involved in a sheared base pair interaction. The 2′-OH of the first loop residue is involved in a hydrogen bond with N7 and possibly the 6-amino/oxo groups of the third loop residue. The 2-amino and N7 protons of the first loop residue are hydrogen bonded to the 5′-phosphate of the fourth loop residue. The base of the second loop residue is flipped outside of the loop and is involved in a stacking interaction with the third and fourth loop residues. The direction of the phosphate backbone is flipped between the first and second loop residues, and the pucker of the second loop residue is 2′-endo.

side residue in an otherwise all-RNA oligonucleotide as substrates for RTA.

Differences between 2′-deoxy- and ribonucleosides are not restricted to the missing hydroxyl group. The absence of the 2′-OH results in differences in the equilibrium sugar puckers between 2′-deoxyribonucleosides and ribonucleosides, with 2′-deoxyribonucleosides adopting primarily a 2′-endo conformation and ribonucleosides adopting a 3′-endo conformation (*9*). The constraints of having a 2′-OH also result in a cost for sampling other sugar conformations that is larger than that of its 2′-deoxy counterpart (*10*). To explore this change in sugar pucker as well as to determine what aspect (H-bond donation or acceptance) of the missing 2′-OH was responsible for the observed effects, RNA−OMeNA hybrid substrate analogues containing single 2′-methoxyribonucleosides in an otherwise all-RNA stem−loop substrate were synthesized and kinetically characterized as RTA substrates. 2′-Methoxyribonucleosides have the advantage of an RNA-like sugar pucker, and the methoxy group also serves as a hydrogen bond acceptor. However, they have a relatively bulky methyl group which can disrupt close contacts and prevent H-bond donation.

RTA substrates belong to the GNRA family of unusually stable tetraloops in which N is any nucleoside and R is any purine. This family of stem−loops has melting temperatures 10−15 °C higher than those of similar stem−loops that are not members of this family (*11*). Figure 1 shows a cartoon of a GNRA stem−loop with some of the interactions that are involved in loop stability. Our kinetic study will attempt to characterize the binding and TS stabilizing components of each substrate's interaction with RTA. RTA's K_m closely approximates the thermodynamic dissociation constant for both RNA and DNA stem−loops and is therefore a measure of the energetic cost for transfer of the substrate from its solvent-bound state to the enzyme-bound state. This energetic cost can be altered by changing the affinity of the enzyme for the mutant substrate, or by changes in the interactions of the substrate with the solvent. Methods that monitor the substrate's solution stability are useful for determining the mechanism of binding. The loop-stabilizing interaction that is most relevant to this work is the interaction of the 2′-OH of the first loop residue via a hydrogen bond with N7 and possibly 6-amino/oxo groups of the third loop residue (Figure 1). Mutation of this first residue of the loop to 2′-deoxyguanosine destroys this interaction. DNA GNRA stem−loops are also unusually stable (*12*). Thus, the 2′-OH interaction is not crucial to loop stability (*13*) and kinetic properties will reflect differences other than loop energetics.

Efficient catalysis with large substrates typified by stem−loop or ribosomal RNAs presents unique challenges. Obtaining site specificity requires that the enzyme have energetically favorable interactions with enough functional groups to reach the transition state but few enough to efficiently release products. In the analysis by Jencks (*14*), the potential binding energy available in a single glucose molecule alone is in the range of 10−20 kcal/mol. If the upper limit of this binding energy was optimized in the formation of the enzyme−substrate complex, turnover would exceed the lifetime of the enzyme. This potential binding energy for an RNA 4mer loop sequence is much greater and the interactions must be optimized to achieve the reported k_{cat} of 30 s^{-1} achieved by RTA on eukaryotic ribosomes.

The members of the GNRA family of stable tetraloops have similar tertiary structures (*15*) and are the most common loops in large RNAs (*16*). For example, in the *Escherichia coli* 16S rRNA, there are 17 tetraloops, and nine of these are in the GNRA class. The trend is similar for other large bacterial and eukaryotic RNAs. Yet RTA depurinates only the single ricin−sarcin GAGA loop of eukaryotic and RNAs. RTA uses binding interactions for specificity and couples the optimization of binding interactions to transition state stabilization. Here we use substrate specificity experiments to establish these interactions with minimal stem−loop substrates.

MATERIALS AND METHODS

Oligonucleotide Purification and Characterization. DNA oligonucleotides were synthesized on an Applied Biosystem 391 DNA synthesizer in the trityl-off mode at a 1 μmol scale. Cleavage and deprotection were carried out by incubation in a 3:1 (v/v) NH_4OH/EtOH solution at 55 °C for 3 h. RNA and hybrid (DNA and RNA) oligonucleotides were purchased (2′-ACE-protected) from Dharmacon Research Inc. and were deprotected essentially as described in the Dharmacon manual, except that a 30 min heating protocol was used instead of the recommended 60 min protocol. After deprotection, the oligos were purified using an Xterra C18 reverse phase column using 50 mM ammonium acetate and a linear gradient of methanol. The integrity and identity of the resulting oligonucleotide were determined using MALDI-TOF mass spectroscopy and enzymatic digestion. The enzymatic digestions were carried out essentially as described previously (*5*); briefly, 100 μL of a 3−10 μM solution of each oligonucleotide was treated with approximately 1 unit

each of *Crotalus adamanteus* snake venom phosphodiesterase and calf intestinal phosphatase and incubated overnight at 37 °C. The digests were analyzed by injection on a reversed phase C18 analytical column (WAT011802) eluted using isocratic conditions in 50 mM ammonium acetate (pH 5.0) and 5% MeOH. Nucleoside and deoxynucleoside standards were used to determine the relative amounts of each component in the oligonucleotide digest.

Kinetic Characterization of the Intrinsic Chemical Reactivity of Adenosine and Deoxyadenosine. Adenosine (1 mM) and deoxyadenosine (100 μM) in 10 mM potassium citrate (pH 4) and 1 mM EDTA were heated at 95 °C. The amount of adenine released was determined by HPLC. Reactions were only allowed to proceed to <50% completion for determination of first-order rates.

Estimation of Errors and Significance of Data. RNA, DNA, and RNA−DNA hybrid stem−loops characterized in this study were heated to 94 °C for 1 min, cooled on ice, and incubated at 37 °C for at least 15 min before the addition of RTA. The relative kinetic constants in experiments that were carried out simultaneously had typical variations of ±20%. The kinetic parameters reported here are results from individual substrate saturation experiments. The results shown in the tables are the best experiments for representing the trends seen in multiple experiments. The errors shown are the errors of the best fit of the data from the representative experiments.

In this analysis, the Michaelis constant is assumed to be a dissociation constant. Earlier characterization of RTA showed that RTA has <5% forward commitment for both RNA and DNA stem−loops (*8*). Catalysis is slow relative to substrate equilibration.

Kinetic Characterization of RTA Activity on Stem−Loop Substrates. Assays were carried out essentially as described previously (*5*), except that the reactions were quenched by addition of potassium phosphate (pH 8.0) to a final concentration of 100 mM. The protein is inactive against stem−loop substrates under these high-salt and -pH conditions. Identical conditions were used for characterization of all oligonucleotides. Oligonucleotide concentrations ranged from 10 nM to 300 μM, and the amount of RTA used was always <15% of the lowest substrate concentration. The maximal amount of conversion to product was always <10% of the total initial substrate concentration. RTA was shown to be able to catalyze multiple turnovers on all the substrates characterized in this study. Under these conditions, initial reaction rates were observed when using multiple-time-point analysis.

Ricin A-Chain Purification. RTA has been cloned into the pET-3D expression vector without N-terminal or C-terminal extensions and was grown and expressed using a modification of the published procedure (*17*). Briefly, *E. coli* BL21-(DE3) cells (Stratagene) transformed with the plasmid were grown in 2× LB medium containing 0.2% glucose at 37 °C to an OD_{600} of 0.5−0.8, induced with 50 μM IPTG, and then grown at 25 °C overnight (~9 h). Cells were pelleted by centrifugation, frozen at −70 °C, thawed on ice, and resuspended in a minimal volume of resuspension buffer [100 mM KCl, 50 mM potassium phosphate (pH 7.4), 0.2 mM PMSF, and 0.1 mg/mL lysozyme]. The mixture was incubated on ice for 30 min, and then the cells were disrupted using a French pressure cell. The crude extract was centrifuged at 12 000 rpm for 30 min, and then a 25% $(NH_4)_2SO_4$ fractionation was carried out with the supernatant. The resulting mixture was centrifuged at 12 000 rpm for 30 min, and then a 40% $(NH_4)_2SO_4$ cut was done on the resulting supernatant. The pellet from the 40% $(NH_4)_2SO_4$ cut was dialyzed twice against 50 mM potassium phosphate (pH 8.0) and 0.1 mM EDTA and loaded on a fast-Q anion exchange column. RTA does not bind the column and so elutes before the start of the gradient. The RTA peak was pooled, concentrated, and dialyzed against 50 mM sodium acetate (pH 4). The yield of RTA by this method is usually ~10−25 mg/L of culture, and the protein is ~96% pure.

DNase activity was removed by dialysis against 5 mM potassium phosphate (pH 6.5), application to a CM-Sepharose column (Amersham), and elution with 300 mM KCl. The protein elutes at ≈260 mM KCl. RNase activity was removed by applying RTA (≈1 mg/mL) in 50 mM sodium acetate, 0.1 mM EDTA, and 1 mM DTT, on a uridine 2′,5′- and 3′,5′-diphosphate agarose column at a solution-to-column volume ratio of 10:1. RTA does not bind the column and is eluted with a minimal amount of the same buffer. The RTA in this study was cloned from a single castor bean and overexpressed in *E. coli*. The enzyme contains a Val81Met amino acid variant compared to the sequence reported previously (*18*, *19*). Kinetic characterization with A-10 indicated that the k_{cat} and K_m values are 1.5 min^{-1} and 1.3 μM, respectively. Earlier characterization of A-10 activity using commercial preparations of RTA reported k_{cat} values of 2−7 min^{-1} and K_m values of 2−5 μM (*5*, *20*).

Oligonucleotide Thermal Denaturation. Solutions containing 1−30 μM solutions of each oligonucleotide in 10 mM potassium citrate (pH 4.0) and 1 mM EDTA were heated while UV spectra were recorded. The samples were heated at a rate of 0.5 °C/min and held at each temperature for 2 min before the absorbance was recorded. Plots of absorbance versus temperature were generated, and the melting temperature was obtained by taking the derivative of the curve and assuming a two-state model.

RESULTS

Kinetic Characterization of the Intrinsic Chemical Reactivity of Adenosine and Deoxyadenosine in the Depurination Reaction. The intrinsic reactivity of adenosine and deoxyadenosine were established under the RTA assay conditions in 10 mM potassium citrate (pH 4) and 0.1 mM EDTA. The rate of deoxyadenosine depurination was 400 times that of adenosine at 95 °C. This is in reasonable agreement with reported rates of adenosine- versus deoxyadenosine acid-catalyzed depurination at pH 1.0 (*6*). The mechanism for acid-catalyzed depurination of adenine nucleosides is dissociative, similar to the transition state established for RTA (*8*). Hence, it is of interest to compare the relative rates of depurination of adenine nucleosides in solution to those obtained on the enzyme.

Oligonucleotide Thermal Denaturation. RNA−DNA hybrid oligonucleotides characterized in this study exhibited clear two-state behavior in their melting transitions and their melting temperatures (53 ± 1 °C) did not vary with concentration in the ranges that were tested (not shown). This is consistent with the existence of the oligonucleotides primarily as unimolecular hairpins in solution. The differ-

Table 1: Kinetic Characterization of DNA−RNA Hybrid Stem−Loops as Substrates for RTA[a]

substrate	k_{cat} (min^{-1})	K_m (μM)	k_{cat}/K_m (M^{-1} s^{-1})	relative k_{cat}	relative K_m	relative k_{cat}/K_m
dA12	0.5 ± 0.04	8.4 ± 1.2	9.9×10^2	1	1	1
dA12_5G	0.9 ± 0.1	5 ± 1.4	3.0×10^3	1.8	0.59	3.0
dA12_6A	0.09 ± 0.003	15.2 ± 1.7	9.4×10	0.17	1.8	0.1
dA12_7G	0.5 ± 0.04	10 ± 2.6	8×10^2	0.96	1.2	0.8
dA12_8A	0.23 ± 0.02	9.4 ± 3.3	4.1×10^2	0.47	1.1	0.42

[a] These are DNA−RNA hybrid GAGA tetraloop stem−loops containing a single ribonucleoside residue in an otherwise all-DNA oligonucleotide. See Figure 2 for structures.

Table 2: Kinetic Characterization of RNA−DNA Hybrid Stem−Loops as Substrates for RTA[a]

substrate	k_{cat} (min^{-1})	K_m (μM)	k_{cat}/K_m (M^{-1} s^{-1})	relative k_{cat}	relative K_m	relative k_{cat}/K_m
A12	101 ± 7	2.7 ± 0.4	6.2×10^5	1	1	1
A12_5dG	0.32 ± 0.05	0.7 ± 0.3	7.5×10^3	0.003	0.26	0.012
A12_6dA	1660 ± 380	32 ± 11	8.6×10^5	17	12	1.4
A12_7dG	0.63 ± 0.04	0.9 ± 0.2	1.2×10^4	0.006	0.33	0.019
A12_8dA	3.3 ± 0.18	5.7 ± 1.1	9.5×10^3	0.03	2.1	0.015

[a] These are RNA−DNA hybrid GAGA tetraloop stem−loops containing a single deoxyribonucleoside residue in an otherwise all-RNA oligonucleotide. See Figure 3 for structures.

ences in T_m values between classes of oligonucleotides differing by one hydroxyl group were not significant within the limits of error of the experiment. The stability of different stem−loops was established to determine if differences in melting temperatures between oligonucleotide analogues could account for the changes observed in kinetic parameters. T_m reflects hairpin stability, an equilibrium characteristic. No relationship was found between stem−loop stability, k_{cat}, and K_m values.

Kinetic Characterization of DNA−RNA Hybrid 12mers Containing Single Ribonucleoside Residues. The DNA 12mer dA12 is depurinated 200-fold slower than its RNA stem−loop counterpart (Tables 1 and 2). DNA−RNA hybrid stem−loops containing a single ribonucleoside residue in an otherwise all-DNA oligonucleotide were studied as substrates for RTA, to probe the basis for the reactivity difference (Figure 2). The largest effect was a 5-fold decrease in k_{cat} at the adenine depurination site (Table 1).

Introduction of a 2′-OH at the first position of the d[GAGA] tetraloop of dA12 results in a 3-fold increase in the k_{cat}/K_m ratio. Structural characterization of GAGA stem−loops shows that in RNA stem−loops of this family, this 2′-OH forms a hydrogen bond with N7 of guanosine at the third loop residue (Figure 1). This structure is supported by crystallographic and NMR studies (*21*). If this is the catalytically relevant loop conformation, it would be expected that placing an RNA residue at the 5 position (dA12_5G; see Figure 2) would restore this interaction to provide an increase in the catalytic rate. Although both k_{cat} and K_m are more favorable in dA12_5G than in dA12, the k_{cat}/K_m of 3.0×10^3 M^{-1} s^{-1} for dA12_5G is much less than that of A12 which is 6.2×10^5 M^{-1} s^{-1} (Tables 2 and 3).

Introduction of a 2′-OH at the second position of the d[GAGA] tetraloop in dA12_6A results in a 10-fold decrease in the k_{cat}/K_m ratio. This change in catalytic efficiency is due to changes in both k_{cat} and K_m, although the more significant (5-fold) change is in k_{cat}. A 2′-OH at the depurination site of the GAGA loop restores the RNA nature of the site but also introduces a more chemically stable bond (400-fold; see above). Consequently, it is expected that replacement of the reactive deoxyadenosine residue with adenosine would result in a decrease in reactivity. However, the (5-fold) change is not consistent with the intrinsic chemical reactivity of adenosine and deoxyadenosine (400-fold). These results suggest that RTA is >40 times (k_{cat}) more adept at enhancing the rate of depurination of an adenosine at the depurination site than a deoxyadenosine at the same site when the stem−loop is DNA. The mechanism for this preference is not yet known. While the doubling of K_m [K_m-(dA12_6A)/K_m(dA12)] (Table 1) is a small factor, it suggests that the 2′-hydroxyl at the depurination site is not a major recognition element for forming the Michaelis complex.

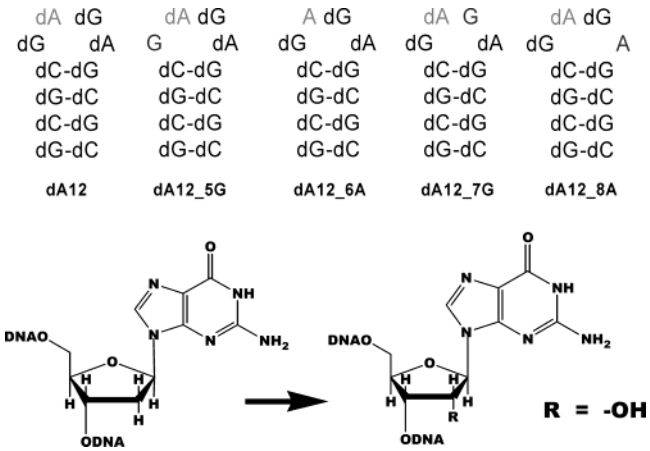

FIGURE 2: Stem−loop DNA structures and the nucleoside modifications of RTA substrates characterized in Table 2. The site of adenine depurination is at position 6 (second base in the loop), and the positions of the other modified nucleotides are indicated in the oligonucleotide structures. The parent oligonucleotide for these substrates is dA12.

Introduction of a 2′-OH at the fourth position of the d[GAGA] tetraloop of dA12 (dA12_8A) results in a 2-fold decrease in the k_{cat}/K_m ratio with the main contribution to this decrease from a decrease in k_{cat}. Structural characterization of GAGA tetraloop stem−loops has shown that in RNA stem−loops of this type, this 2′-OH is pointing into the solution. Unlike the 2′-OH of the first loop position, it is not involved in any conserved hydrogen bonding interactions with other members of the loop.

Introduction of a 2′-OH at the third position of the d[GAGA] tetraloop of dA12 does not result in any significant change in k_{cat}/K_m, k_{cat}, or K_m. Structural characterization of GAGA tetraloop stem−loops has shown that in RNA stem−loops of this class, this 2′-OH is pointing out into the solution. This finding is consistent with the lack of a significant effect on catalysis.

DNA stem-loops are 200-fold less reactive to RTA than RNA, and restoring RNA at the depurination site does not return the substrate activity. Therefore, other 2-hydroxyl groups are implicated in the stem−loop structure required for robust RTA activity. The effects of 2′-OH substitutions of the DNA stem−loop are much smaller than the effects of 2′-H substitutions of the RNA stem−loop as shown below.

Kinetic Characterization of RNA−DNA Hybrid 12mers Containing Single Deoxyribonucleosides in an RNA Context. RNA−DNA hybrid GAGA tetraloop stem−loops containing

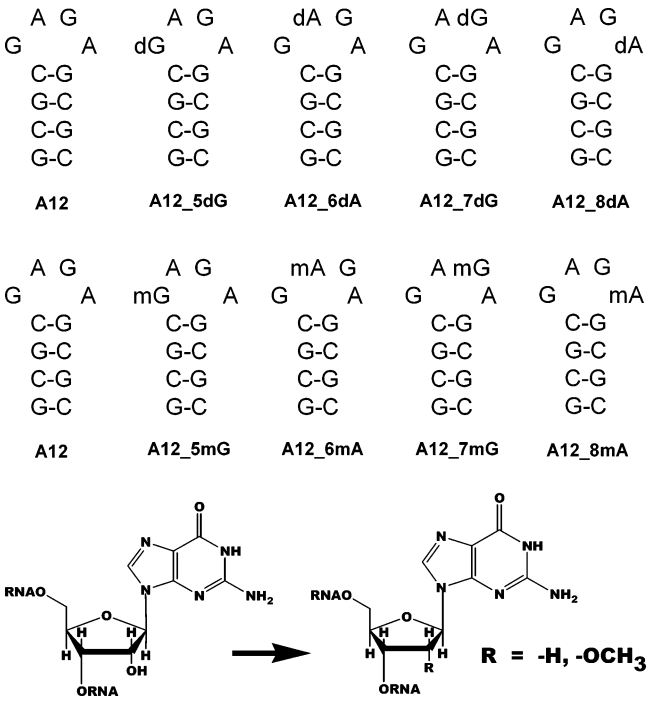

FIGURE 3: Stem−loop RNA structures and the nucleoside modifications of RTA substrates characterized in Tables 3 and 4. The site of adenine depurination is at position 6 (second base in the loop), and the positions of the other modified nucleosides are indicated in the oligonucleotide structures. The parent oligonucleotide for these substrates is A12.

a single deoxyribonucleoside residue in an otherwise all-RNA oligonucleotide were studied as substrates for RTA. These substrates are intended to map the sites responsible for the 200-fold change in catalytic activity between A12 and dA12. Every substitution causes large effects on catalysis (Table 2). Deletion of any 2′-OH in the GAGA loop alters k_{cat} from a 300-fold decrease to a 17-fold increase. This result is surprising considering that three of the four hydroxyls are >12 Å from the reactive adenine and that the last three hydroxyls of the loop have no apparent role in loop stabilization (Figure 1).

The catalytic role of the 2′-OH of the first loop residue was studied by characterization of A12_5dG (Figure 3 and Table 2). Deletion of this 2′-OH results in a 330-fold decrease in k_{cat} and an 80-fold decrease in the k_{cat}/K_m ratio. It is noteworthy that the decrease in catalytic efficiency comes solely from k_{cat} with K_m decreasing 4-fold. The decreased k_{cat} reflects the increased energetic cost for formation of the transition state, while the decreased K_m indicates that transfer of the substrate from solution to its bound state for this analogue (A12_5dG) is 0.85 kcal more favorable than for A12. There is no change in the melting temperature between A12 and A12_5dG, suggesting similar solution properties. Thus, binding energy must arise from more favorable RTA stem−loop interactions. Structural characterization of RNA GAGA tetraloop stem−loops shows this 2′-OH is involved in a hydrogen bond with N7 of the third loop residue, guanosine 7 (Figure 1), indicating a clear role in the solution structure of the loop. Deletion of the 2′-OH increases the energetic cost for adopting this specific conformation and causes a decrease in the catalytic rate.

The second residue of the GAGA loop is the residue at which depurination occurs. Deletion of the 2′-OH at this position increases k_{cat} 16.6-fold but also increases K_m by a similar value (12-fold) for almost no change in k_{cat}/K_m. The effects of k_{cat} and K_m on this change in catalytic efficiency are in opposite directions. These constants indicate a clear involvement of this 2′-OH in binding and stabilization of the ground state. The increase in catalytic productivity is due to a 16-fold (1.71 kcal/mol) decrease in the transition state barrier. However, the significance of the k_{cat} change requires analysis of the effect of the 2′-OH for the intrinsic reactivity of adenosine to depurination. The change of this residue to 2′-deoxyadenosine increases the chemical reactivity 400-fold. Since the k_{cat} increases only 16-fold, RTA is 25-fold more adept at depurination of adenosine from A12 than of deoxyadenosine in A12_6dA. Even though the 2′-OH of this residue is destabilizing for formation of the oxacarbenium ion intermediate, it is being used by the protein to reduce the height of the TS barrier by 2 kcal/mol. Earlier characterization of RTA activity on short RNA stem−loops using catalytic amounts of RTA showed no catalytic activity ($<10^{-5}$ min^{-1}) at neutral pH (*5*). The biological relevance of RTA catalysis on short stem−loops suggests that pK_a values of groups on RTA or the rRNA substrate differ from those in the stem−loop case. However, the catalytic rate of depurination of A12_6dA is comparable to the rate of turnover of RTA on ribosomes. Thus, A12_6dA fully exploits RTA's catalytic potential, albeit with a chemically destabilized substrate. This finding establishes short stem−loops as a robust system for studying RTA's catalytic mechanism.

The 2′-OH of the third loop residue is oriented toward the solvent in stem−loop structures (Figure 1). It was studied by characterization of A12_7dG and results in a 167-fold reduction in k_{cat}. The effect of K_m on k_{cat}/K_m is in the opposite direction. The magnitude and direction of the effects of this deletion are similar to those at the first loop residue, and the same observations apply. Briefly, the deletion of the 2′-OH group results in a more stable enzyme−substrate complex and a higher transition state barrier. Similar magnitudes of the effects for deletion of the first and third loop residue 2′-hydroxyls suggest that the loss in catalytic productivity upon deletion of the 2′-hydroxyls of these residues is through a common tertiary structure which requires both 2′-OH groups of the first and third loop residues.

Deletion of the fourth loop hydroxyl (A12_8dA) reduces k_{cat}/K_m by 60-fold. This reduction is dominated by a 2.2 kcal/mol decrease in the turnover rate, to 3% of that of A12. The small (2-fold) increase in K_m indicates that binding is less favorable. The structure of the canonical GNRA loop shows the 2′-OH pointing into the solvent and suggests that this 2′-OH does not play a direct role in loop stabilization. This result is also consistent with this 2′-OH affecting catalysis via changes in the backbone phosphodiester structure or direct binding of RTA.

Kinetic Characterization of RNA−OMeNA Hybrid 12mers Containing Single 2′-O-Methoxyribonucleosides in an RNA Context. Replacement of the first loop ribonucleoside with 2′-*O*-methoxyribonucleoside (A12_5mG) results in an approximately 0.8×10^4-fold reduction in k_{cat}/K_m (Table 3 and Figure 3). This reduction is dominated by a 0.8×10^4-fold reduction in k_{cat} with no increase in K_m. Deletion of this hydroxyl results in a tighter binding substrate (A12_5dG). Methylation quadruples the size of the 2′-substituent and

Table 3: Kinetic Characterization of RNA−MeNA (2′-*O*-Methoxy Nucleic Acid) Hybrid Stem−Loops as Substrates for RTA[a]

substrate	k_{cat} (min^{-1})	K_m (μM)	k_{cat}/K_m (M^{-1} s^{-1})	relative k_{cat}	relative K_m	relative k_{cat}/K_m
A12	101 ± 7	2.7 ± 0.4	6.2×10^5	1	1	1
A12_5mG	0.08 ± 0.003	2.9 ± 0.6	4.6×10^2	0.0008	1.1	7.5×10^{-4}
A12_6mA	>4	>300	4.5×10^2	>0.04	>100	7.3×10^{-4}
A12_7mG	0.28 ± 0.01	6.3 ± 1.4	7.5×10^2	0.003	2.3	1.2×10^{-3}
A12_8mA	5.1 ± 0.8	9.7 ± 4.7	8.8×10^3	0.05	3.6	1.4×10^{-2}

[a] These are RNA−MeNA hybrid GAGA tetraloop stem−loops containing a single 2′-*O*-methoxy ribonucleoside residue in an otherwise all-RNA oligonucleotide.

Table 4: Kinetic Characterization of RNA−DNA Hybrid Stem−Loops as Substrates for RTA[a]

substrate	k_{cat} (min^{-1})	K_m (μM)	k_{cat}/K_m (M^{-1} s^{-1})	relative k_{cat}	relative K_m	relative k_{cat}/K_m
A12	101 ± 7	2.7 ± 0.4	6.2×10^5	1	1	1
A12_5dG_7dG	>0.04	>100	6.6	$>4 \times 10^{-4}$	>37	1.1×10^{-5}
A12_5dG_8dA	0.6 ± 0.1	1.8 ± 0.35	5.5×10^3	0.006	0.67	0.9×10^{-2}

[a] The sequences of the two hybrid oligonucleotides that were tested are 5′-GCGC-dG-A-dG-A-GCGC-3′ and 5′-GCGC-dG-AG-dA-GCGC-3′.

prohibits donation of an H-bond from the 2′-hydroxyl. Either 2′-methylation or 2′-deoxy at the first loop position (A12_5dG or A12_5mG, respectively) results in similar increases in the transition state barrier but reduction of the binding barrier, suggesting that donation of an H-bond from the 2′-OH of G5 is essential for efficient catalysis but not binding.

Replacement of the depurination site 2′-hydroxyl with a 2′-*O*-methoxyribonucleoside (A12_6mA) also results in an approximately 0.8×10^4-fold reduction in catalytic productivity, k_{cat}/K_m (Table 3). A linear increase in the turnover rate with increasing substrate concentration was observed without reaching saturation at higher substrate concentrations. On the basis of the results obtained at the highest substrate concentration of A12_6mA (300 μM), it is clear that the K_m of this stem−loop is >100-fold higher than that of the all-RNA substrate. This lower limit for K_m together with the k_{cat}/K_m value gives a lower limit for k_{cat} of >4% of that of A12. The preference for the hydroxyl group as opposed to the methoxy group at this position is <1.4 kcal/mol, while the energetic cost for binding is >3 kcal/mol. Hyperconjugation from the 2′-*O*-methoxy substituent results in a lower barrier for the S_N1 chemical transition state. In the stem−loop RNA structure, the 2′-hydroxyl is solvent-exposed, and would not be expected to alter the stem−loop structure. However, the 2′-hydroxyl group is an important H-bond site in the catalytic sites of *N*-ribosyltransferases, and the poor binding of A12_6mA suggests that an enzymatic group hydrogen bonds to the 2′-hydroxyl at the depurination site. Even close packing without H-bond formation would be disrupted by the bulk of the methyl group. Thus, close interaction of RTA with the 2′-OH is implicated.

Replacement of the third loop 2′-ribonucleoside with a 2′-methoxyribonucleoside (A12_7mG) results in an 800-fold reduction in the relative k_{cat}/K_m (Table 3). This decrease is dominated by a 360-fold reduction in k_{cat}. There is also a 2.3-fold increase in K_m. The methoxy substitution destabilizes the ground state complex by 0.5 kcal/mol and the transition state complex by 3.8 kcal/mol relative to A12. In addition to the steric bulk of the 2′-methoxy group, the 2′-methoxy group is unable to donate a hydrogen bond. The 2′-hydroxyl of stem−loop RNA is oriented toward the solvent and is available for catalytic site interactions. These results demonstrate that the 2′-hydroxyl interacts with RTA to facilitate transition state complex formation with little effect on forming the Michaelis complex.

Replacement of the fourth 2′-ribonucleoside of the loop with a 2′-methoxyribonucleoside (A12_8mA) results in a reduction of k_{cat}/K_m to 1.4% of that of A12. This decrease is dominated by a decrease in the turnover rate (k_{cat}) ($\Delta\Delta G$ = 1.9 kcal/mol) as opposed to a 3.6-fold ($\Delta\Delta G$ = 0.83 kcal/mol) change in K_m. This hydroxyl group in the RNA stem−loop is solvent-exposed and available for catalytic site interactions. The large change in k_{cat} as opposed to the drop in K_m suggests that RTA has additional binding interactions with this 2′-hydroxyl group formed in the transition state. The impact, in terms of the relative k_{cat}/K_m of the 2′-O-methoxy substitution, is lower in magnitude at this position than at the other three loop positions. This difference may reflect this residue as the most distant of the loop 2′-hydroxyls from the depurination site.

Kinetic Characterization of the Additivity of 2′-OH Energetic Contributions. To determine if the energetic contributions of individual 2′-OH groups are additive or cooperative, we kinetically characterized substrates that had two deoxyribonucleoside residues in an otherwise all-RNA context. A12_5dG_7dG showed only a linear increase in reaction rate with increasing substrate concentration up to the highest concentration that was tested. Limits on k_{cat} are ≥0.04 and for K_m are >100 μM to provide a limit of 10^5-fold reduction in k_{cat}/K_m (Table 4). Reduction in k_{cat}/K_m from the double mutations is approximately the product of the individual ones (compare Tables 3 and 5); thus, both changes are expressed in the double mutant, supporting individual, independent, and important contacts for catalytic function. One site is implicated in loop stabilization and the other in a catalytic site contact, yet both contribute independently to catalysis. However, unlike the k_{cat}/K_m, changes in the k_{cat} and K_m values of A12_5dG_7dG are not the product of the individual changes in k_{cat} and K_m.

To determine the generality of these trends, we kinetically characterized A12_5dG_8dA (Table 4). In the case of this substrate, the reduction in k_{cat}, K_m, and k_{cat}/K_m from the double mutations is approximately the product of the individual ones (compare Tables 3 and 5), again supporting

Table 5: Kinetic Characterization of RNA−DNA Hybrid Stem−Loops as Substrates for RTA[a]

substrate	k_{cat} (min^{-1})	K_m (μM)	k_{cat}/K_m (M^{-1} s^{-1})	relative k_{cat}	relative K_m	relative k_{cat}/K_m
A12	101 ± 7	2.7 ± 0.4	6.2×10^5	1	1	1
A12_dGAGA	2.9 ± 0.3	20 ± 5	2.4×10^3	0.03	7.6	4×10^{-3}
dA12_GAGA	0.1 ± 0.02	10 ± 4	1.7×10^2	0.001	3.7	2.7×10^{-4}
dA12	0.5 ± 0.04	8.4 ± 1.2	9.9×10^2	1[b]	1[b]	1[b]
dA12_GAGA	0.1 ± 0.017	10 ± 4	1.7×10^2	0.2[b]	1.2[b]	0.17[b]
A12_dGAGA	2.9 ± 0.3	20 ± 5	2.4×10^3	5.8[b]	2.4[b]	2.4[b]

[a] The sequences of the two hybrid oligonucleotides that were tested are 5′-GCGCd[GAGA]GCGC-3′ and 5′-d(GCGCr[GAGA]GCGC)-3′. [b] Obtained by comparison to the value of dA12.

individual, independent, and important contacts for catalytic function.

Kinetic Characterization of the Role of the Stem in RTA Catalysis. The role of the stem in RTA catalysis was examined with two chimeras, A12_d[GAGA] and dA12_GAGA. The k_{cat}/K_m of RTA with an RNA stem and a DNA loop (A12_d[GAGA]) is 0.4% of that of an all-RNA loop (Table 5). This loss of catalytic efficiency is dominated by the contribution from k_{cat} but also reflects a 7.4-fold increase in K_m. The trend is the same for a construct with a DNA stem and an RNA loop, dA12_GAGA. Its relative k_{cat}/K_m is reduced 3740-fold from that of A12, even though this oligonucleotide has all the loop functional groups found in A12. These losses in substrate function emphasize the context dependence of the energetic signatures of the loop hydroxyls. The structural mechanism for the differences between dA12_GAGA and A12 is not clear, but implies that their stems adopt different geometries.

Table 6: Energetic Contribution[a] of the Respective Hydroxyl Group Characterized Using Each Indicated Mutant

substrate	relative K_m	relative k_{cat}	GS binding energy (kcal/mol)	TS total binding energy (kcal/mol)	additional TS binding energy (kcal/mol)
A12_5dG	0.26	0.003	0.9	3.8	2.9
A12_6dA	12	17	−1.6	−1.83	−0.2
A12_7dG	0.33	0.006	0.72	3.3	2.6
A12_8dA	2.11	0.03	−0.49	2.3	1.8
dA12_5G[b]	0.59	1.80	−0.34	−0.38	−0.04
dA12_6A[b]	1.80	0.17	0.38	1.15	0.77
dA12_7G[b]	1.2	0.96	0.11	0.03	−0.08
dA12_8A[b]	1.1	0.5	0.07	0.49	0.42

[a] The energetic contributions were obtained by transformation of the respective relative binding or catalytic rates using the equation $\Delta G = \Delta H - T\Delta S = -RT \ln K$. [b] The relative k_{cat} and K_m values were determined relative to dA12, the DNA stem−loop substrate, and not A12, the all-RNA substrate.

DISCUSSION

Stem−loop RNA has the potential for interactions with RTA at the depurination site, at neighboring loop residues, and at the base-paired stem. All of these interactions are shown to influence catalysis by systematic modification of each structural element of a small stem−loop substrate. Contributions to TS stabilization from "remote" sites energetically can be worth as much or more than contributions from nearby atoms. Substrate specificity reveals the energetic landscape of the Michaelis and transition state complexes of RTA during catalysis. The results provide binding and catalytic energies.

RTA Uses 2′-OH Groups Primarily for Catalysis. The expression of RTA binding energies (Table 6) indicates that the binding interactions between RTA and the loop hydroxyls are used to optimize transition state binding (catalysis) and not ground state binding. Alterations in the substrate have a larger energetic impact on the TS complex than on the Michaelis complex (Figure 4). The k_{cat} values vary by up to 10000-fold, while K_m values change by modest amounts. None of the substrate mutations resulted in an increased level of TS stabilization, while some of the mutations resulted in increased levels of binding. The rapid k_{cat} for A12_6dA (Table 2) results from an increased intrinsic reactivity at the depurination site rather than enhanced energy being applied at the transition state. Substrate binding of stem−loop RNAs is proposed to involve numerous weak interactions distributed across the loop and possibly involving the stem. Loss of one or two of these has a minimal impact on binding. In contract, the transition state is formed by a few strong interactions to activate the adenine leaving group and to form the riboxacarbenium ion. The deletion of hydroxyls involved in loop formation (A12_5dG) and in groups available for interaction at the catalytic site, but not directly involved in loop formation (A12_7dG), both resulted in substrates that bound RTA tighter yet resulted in a k_{cat} lower than that of the "wild-type" RNA substrate. These groups play an important role in TS stabilization, but by different mechanisms. Loss of a loop-stabilizing interaction and a catalytic site H-bond reduce k_{cat} equally, and the combined mutation (A12_5dG_7dG) shows additive $\Delta G°$ values as expected for independent processes.

RTA Collectively Uses Its Binding Interactions with the Loop Hydroxyls. Three of the loop 2′-hydroxyls are available for interaction with the catalytic site, while that for G5 is involved in loop stability. If each acts independently, the all-DNA loop, all-RNA stem structure A12_dGAGA would be expected to be a very poor substrate, even though a 2′-deoxy at the depurination site increases k_{cat} by 16-fold. The product of the individual changes predicts a decrease in k_{cat} to 10^{-6} relative to that of A12. However, the k_{cat} of A12-dGAGA is reduced only 35-fold. A major difference in the structures of A12 and A12-d[GAGA] is the rigidity of the phosphodiester structural scaffold. Each single deoxy introduced into A12 is likely to prevent the precise placement of H-bond pairs required to reach the transition state. In contrast, A12_d[GAGA] has a flexible loop permitting it to achieve transition state contacts with all but the missing 2′-hydroxyls.

The Catalytic Signatures of the OH Functional Groups Are Context-Dependent. DNA tetraloops of the GNRA family also form stable stem−loops (*12*) and are substrates for RTA. Although an atomic structure of this class of DNA stem−loops has not been reported, their behavior in solution and their enzymatic specificity suggest that they are structur-

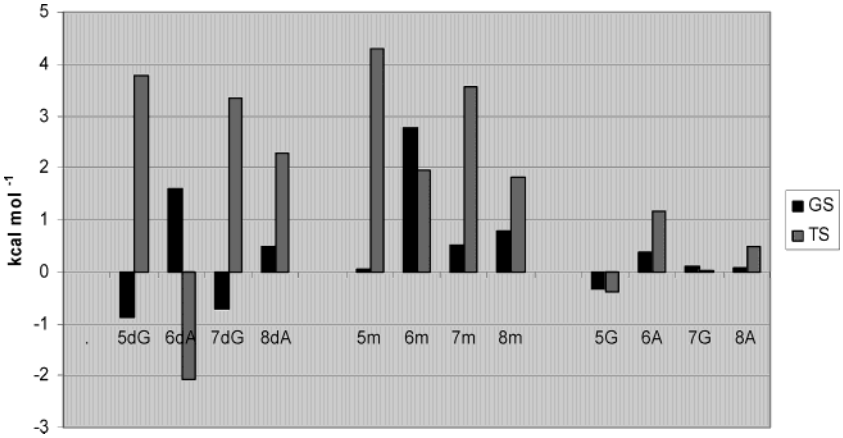

FIGURE 4: The energetic signature of the loop 2′-hydroxyls determined by replacement of the respective functional groups in an RNA context (5dG, 6dA, 7dG, and 8dA), by replacement with 2′-*O*-methoxy functional groups (5m, 6m, 7m, and 8m), and by insertion of 2′-OH groups into a DNA substrate (5G, 6A, 7G, and 8A).

ally similar to their RNA counterparts. DNA stem−loops containing single ribose residues were therefore used to assess the context dependence of the energetic contribution of the loop hydroxyls. Since the energetic impact of each hydroxyl deletion is not conserved with the deletion of more than one additional hydroxyl, the catalytic role of replacing each hydroxyl was explored. Single RNA nucleosides in a DNA context have only small effects upon revival of the substrate properties of stem−loops either in TS stabilizing or in binding effects (Table 1). In contrast, in the context of RNA, characterization of A12__5dG indicates that this 2′-OH contributes 3.78 kcal/mol to the stabilization of the transition state (Table 6). Results obtained from a characterization of its isodimensional DNA counterpart dA12__5G show that in the DNA context, the 5dG 2′-OH contributes only 0.38 kcal/mol to the stabilization of the transition state. The difference in RNA−DNA backbone flexibility is implicated as a major difference in these structures. Transition state analysis for RTA with RNA−DNA stem−loops establishes a rigid ribosyl geometry for RNA and more flexibility in the DNA case (*7*, *8*).

The substrate in the RNA transition state, unlike that for the DNA substrate, passes through an isotopically insensitive rate-limiting step, and the pucker of the reactive nucleoside at the transition state is different for the RNA and DNA reactions. In addition, structural (X-ray crystallographic) and mutational (*22*, *23*) studies of RTA have shown that RTA has a flexible catalytic site, consistent with the ability to affect catalysis on different substrates, but with varied efficiency.

The 2′-OH Groups of the First, Third, and Fourth Residues Mediate Their Normal Effects in Hydrogen Bonds. Kinetic patterns observed in the characterization of the 2′-OH to 2′-H mutants are (a) the preferential expression of the kinetic impact of the mutation in k_{cat} as opposed to K_m, (b) the smallest energetic impact on k_{cat} at the site of chemistry (second loop hydroxyl) followed by the fourth loop residue, and (c) the largest energetic impact on K_m at the site of chemistry which are similar to the effects with the 2′-OH to 2′-OCH_3 mutants. The 2′-OCH_3 nucleosides in an otherwise all-RNA context correct for the differences in sugar pucker between ribo- and deoxyribonucleosides. They also limit interactions to H-bond acceptance at the 2′-position. A limitation of this analysis is that the methyl group will alter loop structure when placed at the 5G position, but in the other positions changes primarily bulk and H-bond potential. The similarity of the kinetic patterns from the 2′-deoxy and the 2′-OCH_3 substrate analogues suggests that altered H-bond donation potential is the major factor. The 2′-OH groups of the first, third, and fourth residues are proposed to mediate their effects in hydrogen bond donation as opposed to hydrogen bond acceptance or sugar pucker. These hydrogen bonds have relatively modest effects in the Michaelis complexes but greater effects on k_{cat}, consistent with them becoming tighter in the transition state. The contribution of the respective 2′-OH groups to the reduction of the catalytic barrier is primarily by optimization of the hydrogen bond angle and/or distance or by transfer of the bond into a more hydrophobic environment (*24*).

Is RTA Acting as a Ribozyme? The pattern seen in this study, where ablation of a neighboring hydroxyl has large negative effects on turnover, is seen in the case of ribozymes when the deleted hydroxyl has a direct role in catalysis, e.g., activation of the water nucleophile. This raises a new question about RNA groups participating in the RTA catalytic mechanism. The phenomenon of distant substrate sites contributing to TS stabilization has been seen in the case of both protein and ribozymes (*24*−*26*) and does not permit mechanistic discrimination. However, there are three trends to suggest that RTA is acting as an enzyme and not a ribozyme. In the *Tetrahymena* ribozyme, the total energetic contribution of each hydroxyl was equal and fully realized in each mutant (*24*, *26*, *27*). Only the partitioning into ground or transition state binding was unique for each hydroxyl. This is not the case for RTA. The total energetic contribution of each hydroxyl as well as its partitioning is unique to each hydroxyl and is more consistent with action as an enzyme. A second property is that the catalytic advantage (k_{cat}/k_{non}) of RTA on these substrates is in the regime of enzymes and not ribozymes. Finally, the intrinsic depurination rate of A12 is extremely slow, and none of the 2′-OH deletions ablates RTA-catalyzed depurination activity.

Binding and Catalysis. Stem−loop mutational analysis reveals two kinds of stem−loop alterations, those that partition to both TS and Michaelis complexes and those that are dominated by k_{cat} effects. Figure 5 illustrates catalytically relevant binding effects that reduce the catalytic barrier by stabilizing the GS and TS (uniform binding) and those that

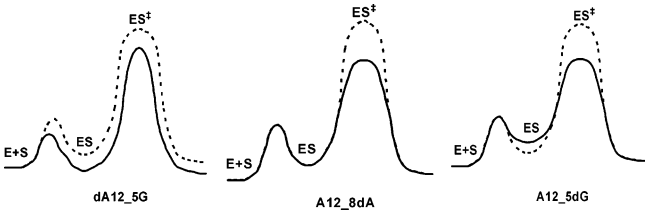

FIGURE 5: Three types of catalytically relevant binding patterns. The first, where the contribution to TS stabilization is (almost) fully realized in the GS, is demonstrated by the 2′-OH of the fifth nucleoside of the substrate mutant dA12_5G. The second, where binding interactions are preferentially realized in the TS by bond optimization, is a pattern demonstrated by the energetic contribution of the deleted 2′-OH of the eighth nucleoside (A12_8dA). The third, binding interactions that are preferentially realized in the TS by relief of a GS destabilizing interaction, is demonstrated by the energetic contribution of the deleted 2′-OH of the fifth nucleoside (A12_5dG).

form favorable interactions only in the TS (specific binding). Reduction of the catalytic barrier by TS binding can be facilitated by destabilization of the GS which contributes to the TS. Three kinds of catalytic and substrate binding effects are represented in the stem−loops (Figure 5). Uniform binding occurs with dA12_5G (Table 6). This 2′-OH forms a bond with RTA that is worth 0.34 kcal/mol in the GS, and the same change is carried into the TS. In A12_5dG and A12_7dG, deletion of their respective 2′-OH groups results in tighter binding, but reduced k_{cat} values relative to that of A12. This pattern is consistent with catalysis by GS destabilization. Weaker substrate binding coupled to an increased k_{cat} in A12_6dA results from the destabilization of the C1′−N9 N-ribosidic bond. In this case, correction of the energetic contribution for the 2′-OH establishes a GS binding which is worsened in the TS, a pattern which is consistent with uniform binding with additional specific binding (bond strengthening) in the TS. A similar pattern is seen in A12_8dA.

RTA Prefers an RNA Stem. RNA stems can adopt both an A-form and B-form stem depending on the sequence and solution conditions (*10*). NMR studies of an RNA 12mer stem−loop with a loop sequence identical to that of A12 showed that its stem adopts an A-type conformation (*28*). One difference between A- and B-form stems is the width of the stem. Increased stem width would result in different end-to-end loop lengths and therefore different spatial locations of functional groups involved in binding or catalysis. The role of the stem was analyzed in the kinetic characterization of dA12-GAGA, containing a DNA stem with the same RNA loop as in A12. The 1000-fold reduction in k_{cat} via a change in only the stem shows a strong preference for an RNA stem. The mechanism by which this preference is mediated is not known and requires structural analysis of both RNA and DNA stem−loops alone and in complex with RTA.

The 2′-OH Groups of GNRA Loops Play No Significant Role in Loop Stabilization. A systematic study of the impact of hydroxyl deletions on the stability of RNA GNRA stem−loops has not been reported. Interactions involved in stabilization of GNRA loops have shown that the energetic contribution of each group to the stability of these loops varies with the position in the loop (*13*). It has also been shown that DNA tetraloops of the GNRA family, although lacking the 2′-OH functional groups, also form stable stem−loops (*12*). Melting curves demonstrate that the 2′-OH groups of the loop riboses play no significant role in loop stability. These results support earlier results which show that loop stability in GNRA loops is mediated by a plastic network of hydrogen bonds (*13*) and may be dominated by other mechanisms such as base stacking.

Implications for Inhibitor Design. Inhibitor design for RTA has the goals of capturing Michaelis complex and transition state interactions. KIE studies of RTA have shown that its reaction stabilizes a highly dissociative S_N1 reaction with formation of a full oxocarbenium ion intermediate. 4-Aza-2′-deoxyribose sugars have been incorporated into stem−loop RNA and used as TS inhibitors of RTA. Substrate specificity shows that RTA interacts with the 2′-OH of this residue for binding and TS stabilization. Hence, a 2′-deoxy residue is not expected to fully capture the TS binding energy of RTA. The energy available from the interaction of this 2′-OH with RTA can be best estimated to be approximately 4 kcal/mol. The difference in binding energy $[-RT \ln(K_i/K_m)]$ between a transition state analogue inhibitor and its substrate analogue is often used as a measure (in comparison to k_{cat}/k_{non}) of the goodness of the inhibitor's approximation of the transition state structure. In earlier work with RTA (*20*), these inhibitors were compared to their all-RNA substrate analogues rather than the RNA−DNA hybrids. Analogues with 2′-deoxy at the depurination site will likely reflect the decreased catalytic efficiency of RTA on 2′-deoxy substrates.

CONCLUSIONS

Substrate specificity studies with RNA−DNA stem−loops establishes that (1) catalysis varies by 10000-fold as a function of stem−loop structure but K_m values change by relatively small factors. Therefore, RTA utilizes the binding energy of the 2′-hydroxyls of the loop nucleosides primarily for catalysis as opposed to stability in the Michaelis complex. (2) Binding and catalysis in RTA depend on interactions with 2′-hydroxyls directly and indirectly involved in loop formation. Catalysis depends on the relatively rigid loop structure of RNA. (3) RNA stems are more efficient than DNA stems at enhancing RTA activity independent of the identity of the loop (RNA or DNA). The enzyme demonstrates the highest catalytic potential on all RNA stem−loops. (4) The 2′-hydroxyl of adenosine at the depurination site is not important for catalysis. The 2′-hydroxyls of guanosines adjacent to the depurination site are more important in stabilizing loop structure and in catalytic site interactions that are necessary for transition state formation. (5) Deoxynucleosides before and after the adenine depurination site lower K_m, and may be significant in the design of stem−loop inhibitors.

REFERENCES

1. Albery, W. J., and Knowles, J. R. (1977) Efficiency and evolution of enzyme catalysis, *Angew. Chem., Int. Ed. Engl. 16*, 285−293.
2. Olsnes, S., and Pihl, A. (1972) Ricin: a potent inhibitor of protein synthesis, *FEBS Lett. 20*, 327−329.
3. Endo, Y., and Tsurugi, K. (1987) RNA N-glycosidase activity of ricin A-chain. Mechanism of action of the toxic lectin ricin on eukaryotic ribosomes, *J. Biol. Chem. 262*, 8128−8130.
4. Endo, Y., Gluck, A., and Wool, I. G. (1991) Ribosomal RNA identity elements for ricin A-chain recognition and catalysis, *J. Mol. Biol. 221*, 193−207.

5. Chen, X. Y., Link, T. M., and Schramm, V. L. (1998) Ricin A-chain: kinetics, mechanism, and RNA stem-loop inhibitors, *Biochemistry 37*, 11605−11613.
6. Garrett, E. R., and Mehta, P. J. (1972) Solvolysis of adenine nucleosides. I. Effects of sugars and adenine substituents on acid solvolyses, *J. Am. Chem. Soc. 94*, 8532−8541.
7. Chen, X.-Y., Berti, P. J., and Schramm, V. L. (2000) Transition-State Analysis for Depurination of DNA by Ricin A-Chain, *J. Am. Chem. Soc. 122*, 6527−6534.
8. Chen, X.-Y., Berti, P. J., and Schramm, V. L. (2000) Ricin A-Chain: Kinetic Isotope Effects and Transition State Structure with Stem-Loop RNA, *J. Am. Chem. Soc. 122*, 1609−1617.
9. Altona, C., and Sundaralingam, M. (1972) Conformational analysis of the sugar ring in nucleosides and nucleotides. A new description using the concept of pseudorotation, *J. Am. Chem. Soc. 94*, 8205−8212.
10. Rich, A. (2003) The double helix: a tale of two puckers, *Nat. Struct. Biol. 10*, 247−249.
11. Antao, V. P., Lai, S. Y., and Tinoco, I., Jr. (1991) A thermodynamic study of unusually stable RNA and DNA hairpins, *Nucleic Acids Res. 19*, 5901−5905.
12. Nakano, M., Moody, E. M., Liang, J., and Bevilacqua, P. C. (2002) Selection for thermodynamically stable DNA tetraloops using temperature gradient gel electrophoresis reveals four motifs: d(cGNNAg), d(cGNABg), d(cCNNGg), and d(gCNNGc), *Biochemistry 41*, 14281−14292.
13. SantaLucia, J., Jr., Kierzek, R., and Turner, D. H. (1992) Context dependence of hydrogen bond free energy revealed by substitutions in an RNA hairpin, *Science 256*, 217−219.
14. Jencks, W. P. (1975) Binding energy, specificity, and enzymic catalysis: the circe effect, *Adv. Enzymol. Relat. Areas Mol. Biol. 43*, 219−410.
15. Correll, C. C., and Swinger, K. (2003) Common and distinctive features of GNRA tetraloops based on a GUAA tetraloop structure at 1.4 Å resolution, *RNA 9*, 355−363.
16. Woese, C. R., Winker, S., and Gutell, R. R. (1990) Architecture of ribosomal RNA: constraints on the sequence of "tetra-loops", *Proc. Natl. Acad. Sci. U.S.A. 87*, 8467−8471.
17. Ready, M. P., Kim, Y., and Robertus, J. D. (1991) Site-directed mutagenesis of ricin A-chain and implications for the mechanism of action, *Proteins 10*, 270−278.
18. Li, S. S., Wei, C. H., Lin, J. Y., and Tung, T. C. (1975) Amino-terminal sequences of the anti-tumor lectin ricin A- and B-chains, *Biochem. Biophys. Res. Commun. 65*, 1191−1195.
19. Cawley, D. B., Hedblom, M. L., and Houston, L. L. (1978) Homology between ricin and *Ricinus communis* agglutinin: amino terminal sequence analysis and protein synthesis inhibition studies, *Arch. Biochem. Biophys. 190*, 744−755.
20. Tanaka, K. S., Chen, X. Y., Ichikawa, Y., Tyler, P. C., Furneaux, R. H., and Schramm, V. L. (2001) Ricin A-chain inhibitors resembling the oxacarbenium ion transition state, *Biochemistry 40*, 6845−6851.
21. Jucker, F. M., Heus, H. A., Yip, P. F., Moors, E. H., and Pardi, A. (1996) A network of heterogeneous hydrogen bonds in GNRA tetraloops, *J. Mol. Biol. 264*, 968−980.
22. Kim, Y., Mlsna, D., Monzingo, A. F., Ready, M. P., Frankel, A., and Robertus, J. D. (1992) Structure of a ricin mutant showing rescue of activity by a noncatalytic residue, *Biochemistry 31*, 3294−3296.
23. Morris, K. N., and Wool, I. G. (1992) Determination by systematic deletion of the amino acids essential for catalysis by ricin A chain, *Proc. Natl. Acad. Sci. U.S.A. 89*, 4869−4873.
24. Shan, S., Yoshida, A., Sun, S., Piccirilli, J. A., and Herschlag, D. (1999) Three metal ions at the active site of the *Tetrahymena* group I ribozyme, *Proc. Natl. Acad. Sci. U.S.A. 96*, 12299−12304.
25. Narlikar, G. J., and Herschlag, D. (1997) Mechanistic aspects of enzymatic catalysis: lessons from comparison of RNA and protein enzymes, *Annu. Rev. Biochem. 66*, 19−59.
26. Silverman, S. K., and Cech, T. R. (1999) Energetics and cooperativity of tertiary hydrogen bonds in RNA structure, *Biochemistry 38*, 8691−8702.
27. Narlikar, G. J., and Herschlag, D. (1998) Direct demonstration of the catalytic role of binding interactions in an enzymatic reaction, *Biochemistry 37*, 9902−9911.
28. Orita, M., Nishikawa, F., Shimayama, T., Taira, K., Endo, Y., and Nishikawa, S. (1993) High-resolution NMR study of a synthetic oligoribonucleotide with a tetranucleotide GAGA loop that is a substrate for the cytotoxic protein, ricin, *Nucleic Acids Res. 21*, 5670−5678.
29. Correll, C. C., Munishkin, A., Chan, Y. L., Ren, Z., Wool, I. G., and Steitz, T. A. (1998) Crystal structure of the ribosomal RNA domain essential for binding elongation factors, *Proc. Natl. Acad. Sci. U.S.A. 95* (23), 13436−13441.

BI0498508